ARR No. E5A05

NATIONAL ADVISORY COMMITTEE FOR AERONAUTICS

WARTIME REPORT

ORIGINALLY ISSUED

January 1945 as
Advance Restricted Report E5A05

THE TWO-DIMENSIONAL INCOMPRESSIBLE POTENTIAL FLOW OVER CORRUGATED AND DISTORTED INFINITE SURFACES

By W. Perl and L. J. Green

Aircraft Engine Research Laboratory
Cleveland, Ohio

NACA

WASHINGTON

NACA ARR No. E5AC5

NATIONAL ADVISORY COMMITTEE FOR AERONAUTICS

ADVANCE RESTRICTED REPORT

THE TWO-DIMENSIONAL INCOMPRESSIBLE POTENTIAL FLOW OVER CORRUGATED AND DISTORTED INFINITE SURFACES

By W. Perl and L. J. Green

SUMMARY

The two-dimensional incompressible potential flow over corrugations and bumps of arbitrary shape is derived by conformal transformation. The results are compared with those obtained by the methods of thin-airfoil theory. Some discussion is included of the flow over bumps that protrude both inward and outward from a wall.

INTRODUCTION

Analyses of the effects of local surface distortions on the drag and the critical speed of airfoils usually begin with a consideration of the two-dimensional incompressible potential flow over a surface having these distortions. In reference 1, for example, the well-known approximate methods of thin-airfoil theory are applied to the calculation of the velocity distribution over periodic corrugations and isolated bumps of sinusoidal shape.

In this paper the ideal flow past such shapes is derived by more exact conformal mapping methods of W. Perl of the NACA staff, particularly inasmuch as the numerical application of these methods is almost as simple as that of the approximate methods of thin-airfoil theory. The results are compared with those obtained by thin-airfoil theory. Some incidental discussion of the conditions at a cusped edge and of the mapping of bumps that extend both inward and outward from a wall is also given.

The analysis in this paper was begun at Langley Memorial Aeronautical Laboratory and completed at the Aircraft Engine Research Laboratory of the NACA at Cleveland, Ohio.

THE FLOW OVER A CORRUGATED SURFACE

Consider a corrugated surface, all the cross sections of which parallel to a fixed plane are the same, having infinite length and arbitrary but periodic shape. It is desired to find the velocity distribution produced along the surface by an ideal incompressible fluid moving parallel to this plane. The free-stream velocity sufficiently far from the corrugation is assumed to be constant, parallel to the axis of periodicity of the cross section, and of magnitude unity.

The problem is solved by finding the conformal transformation between points of the corrugation (actually the cross section), taken as periodic about the θ-axis of a z-plane, and points of a straight line, taken as the ϕ-axis of a ζ-plane (fig. 1). The Cartesian mapping function (CMF), which relates conformally corresponding pairs of points in the two planes, is defined as the vector difference $z - \zeta$ between such pairs of points.
Thus

$$\left.\begin{aligned} z &\equiv \psi + i\theta \\ \zeta &\equiv \psi_0 + i\phi \\ z - \zeta \equiv \Omega - i\epsilon &= (\psi - \psi_0) - i\,(\phi - \theta) \end{aligned}\right\} \qquad (1)$$

The various quantities are defined in figure 1.

The CMF $z - \zeta$ can be regarded as a function that is regular everywhere outside a circle by virtue of the transformations

$$z = \log p' \qquad (2a)$$

$$\zeta = \log p \qquad (2b)$$

in which the coordinates of p' and p are

$$p' = e^{\psi + i\theta}$$

$$p = e^{\psi_0 + i\phi}$$

Equation (2a) transforms the semi-infinite periodic strip in the z-plane, bounded by $\theta = 0$, $\theta = 2\pi$, and the corrugation $\psi(\theta)$, into the entire region outside the p'-plane near circle that corresponds to the corrugation. The corrugation given by the Cartesian coordinates ψ and θ in the z-plane is represented in the p'-plane

by the near circle with polar coordinates e^{ψ} and θ. Similarly, equation (2b) transforms the semi-infinite periodic strip, bounded by $\phi = 0$, $\phi = 2\pi$, and the ϕ-axis ($\psi_0 = 0$), into the entire region outside a unit circle in the p-plane. The CMF $z - \zeta$ becomes a function that is regular everywhere outside the p-plane unit circle and is therefore expressible by an inverse power series

$$z - \zeta = \log (p'/p) = \sum_{1}^{\infty} \frac{c_n}{p^n} \tag{3}$$

wherein the constant term, representing a relative translation between the z-plane and the ζ-plane, has been made zero. The transformation $\log (p'/p)$ in equation (3) has been used in reference 2. On the boundaries equation (3) becomes, with $p = e^{i\phi}$ and $c_n = a_n + ib_n$,

$$\left.\begin{aligned} \psi(\phi) &= \sum_{1}^{\infty} a_n \cos n\phi + \sum_{1}^{\infty} b_n \sin n\phi \\ -\epsilon(\phi) &= \sum_{1}^{\infty} b_n \cos n\phi - \sum_{1}^{\infty} a_n \sin n\phi \end{aligned}\right\} \tag{4}$$

The mapping function $\psi(\phi) - i\epsilon(\phi)$ for a given boundary $\psi(\theta)$ can be obtained from equations (4). Conversely, special families of corrugations are obtained by selecting various harmonics in equations (4); for example, a simple type of corrugation is given by

$$\left.\begin{aligned} \psi(\phi) &= -\frac{\pi T}{2} \cos \phi \\ \epsilon(\phi) &= -\frac{\pi T}{2} \sin \phi \\ \theta(\phi) &= \phi - \epsilon(\phi) = \phi + \frac{\pi T}{2} \sin \phi \end{aligned}\right\} \tag{5}$$

where $T/2$ is the thickness ratio of the corrugation, defined as the total height h (fig. 1) divided by the wave length 2π; the quantity T is thus analogous to the thickness ratio (maximum thickness/chord) of airfoil sections. The members of this family (equations (5)) corresponding to $T = 0$, 0.1, 0.2, and 0.3 are plotted in figure 2 as $\frac{\psi}{\pi T/2}$ against θ.

Once the mapping function of a corrugation is known, the velocity v at any point on the surface is given by the product of the velocity on the straight-line boundary, which is unity, and the stretching factor $\left|d\zeta/dz\right|$ from the straight line to the corrugation; thus, by use of equations (1),

$$v = \left|\frac{d\zeta}{dz}\right| = \frac{1}{\left|\frac{d\psi + i\,d\theta}{i\,d\phi}\right|}$$

$$v = \frac{1}{\sqrt{\left(1 - \frac{d\epsilon}{d\phi}\right)^2 + \left(\frac{d\psi}{d\phi}\right)^2}} \tag{6}$$

For the special family of corrugations given by equations (5) the velocity distribution reduces to

$$\frac{\Delta v}{\pi T/2} \equiv \frac{v-1}{\pi T/2} = \frac{2}{\pi T}\left[\frac{1}{\sqrt{1 + \left(\frac{\pi T}{2}\right)^2 + \pi T \cos\theta}} - 1\right] \tag{7}$$

Figure 3 shows the velocity distributions of members of the special family shown in figure 2. As $T \longrightarrow 0$, ψ and Δv also $\longrightarrow 0$, but both $\frac{\psi}{\pi T/2}$ and $\frac{\Delta v}{\pi T/2} \longrightarrow -\cos\theta$. These limiting values agree with the thin-airfoil results obtained by Allen (reference 1).

In the general case of a given arbitrary corrugation $\psi(\theta)$, the CMF $\psi(\phi) - i\epsilon(\phi)$ can be determined by successive approximations. Suppose, for example, that the zeroth approximation to the corrugation $\psi(\theta)$ is the straight line $\psi_0(\phi) - i\epsilon_0(\phi) = 0$. The first-approximation ordinates $\psi_1(\phi)$, corresponding to a set of evenly spaced ϕ values, are then obtained from the given boundary at the abscissas $\theta_0 = \phi$. The function $\epsilon_1(\phi)$, conjugate to $\psi_1(\phi)$, is determined by harmonic analysis and synthesis in accordance with equations (4). The resulting first-approximation CMF $\psi_1(\phi) - i\epsilon_1(\phi)$ yields the coordinates $\psi_1(\phi)$, $\theta_1(\phi) = \phi - \epsilon_1(\phi)$ of a boundary, which is compared with the given boundary. If the agreement is not satisfactorily close, the procedure is repeated; the second-approximation ordinates $\psi_2(\phi)$ corresponding to the same set of evenly spaced ϕ values, are obtained from the given boundary at the abscissas $\theta_1(\phi) = \phi - \epsilon_1(\phi)$, etc.

As an example of the general procedure and for comparison with the results of Allen (reference 1) in the case of nonnegligible thickness, a cosine corrugation with a thickness ratio of 0.2 was taken as $\psi = -\frac{\pi}{10}\cos\theta$. The zeroth approximation was chosen as the special corrugation T = 0.2 of figure 2. The maximum difference in ordinates of the two surfaces was 30 percent. After the first approximation the maximum difference between the ordinates of the given cosine corrugation and the first-approximation boundary was reduced to about 4 percent. A second and a third approximation further reduced the difference to 1 and 0.25 percents, respectively. The resulting CMF and the velocity distribution for the third approximation are given in table 1. Figure 4 shows this velocity distribution as well as the approximate velocity distribution based on thin-airfoil theory. As was demonstrated by Allen, the approximate velocity distribution is a cosine distribution.

The results obtained by the two methods for a thickness ratio of 20 percent differ appreciably; the maximum difference is about 16 percent of the maximum increment of velocity over the free-stream value. In the range of thickness ratios contemplated by Allen, however, the results of thin-airfoil theory are undoubtedly of sufficient accuracy, as far as incompressible potential flow is concerned.

THE FLOW OVER A BUMP

Consider a surface that is perfectly flat except for an isolated bump or a disturbance of constant chord length and infinite span; assume the flow over the surface to be at right angles to the span and of magnitude unity sufficiently far from the bump. A two-dimensional symmetrical flow is obtained by reflecting the bump in the plane surface. This problem is solved by conformally mapping the symmetrical section, taken in the z-plane, into its axis of symmetry, taken in the ζ-plane. The coordinates in the two planes are (fig. 5)

$$\left.\begin{aligned} z &\equiv x + iy \\ \zeta &\equiv \xi + i\eta \end{aligned}\right\} \tag{8}$$

The CMF $z - \zeta$ becomes a function regular in the exterior of a circle $|p| = R$ as a result of the Joukowski transformation

$$\zeta = p + \frac{R^2}{p}$$

and can be expressed as an inverse power series

$$z - \zeta \equiv \Delta x + i\Delta y = \sum_0^\infty \frac{c_n}{p^n} \tag{9}$$

For corresponding points on the boundaries in the z-, ζ-, and p-planes,

$$\left.\begin{aligned} \Delta x(\phi) &= \sum_0^\infty \frac{a_n}{R^n} \cos n\phi + \sum_0^\infty \frac{b_n}{R^n} \sin n\phi \\ \Delta y(\phi) &= \sum_0^\infty \frac{b_n}{R^n} \cos n\phi - \sum_0^\infty \frac{a_n}{R^n} \sin n\phi \end{aligned}\right\} \tag{10}$$

$$x(\phi) = r \cos \phi + \Delta x(\phi) \qquad (r = 2R)$$

The velocity v at any point of the symmetrical section is the product of the velocity at the corresponding point of the circle $|p| = R$ and the stretching factor $|dp/dz|$. The result is

$$v = \frac{\sin \phi}{\sqrt{\left(\sin \phi - \frac{d\Delta x}{r d\phi}\right)^2 + \left(\frac{d\Delta y}{r d\phi}\right)^2}} \tag{11}$$

The sections under consideration are now assumed to be symmetrical with respect to both the coordinate axes and to have a horizontal tangent at their chordwise extremities on the x-axis. The Fourier series (equations (10)) are thereby simplified; symmetry with respect to the x-axis requires that $b_n = 0$, and symmetry with respect to the y-axis requires the vanishing of even harmonics. Hence,

$$\left.\begin{aligned} \Delta x &= \sum_1^\infty \frac{a_n}{R^n} \cos n\phi \qquad (12a) \\ \Delta y &= -\sum_1^\infty \frac{a_n}{R^n} \sin n\phi \qquad (12b) \end{aligned}\right\} \text{(n odd)}$$

The condition that the section have a horizontal tangent at the chordwise extremities, that is,

$$\frac{dy}{dx} = \frac{\sum_{1}^{\infty} na_n \cos n\phi}{r \sin \phi + \sum_{1}^{\infty} na_n \sin n\phi}$$

be zero for $\phi = 0$, is satisfied if

$$\sum_{1}^{\infty} na_n = 0, \qquad r + \sum_{1}^{\infty} n^2 a_n \neq 0 \tag{13}$$

A simple example of a family of bumps satisfying conditions (13) is given by

$$\left.\begin{aligned} \Delta x &= -\frac{3}{4} T \left(\cos \phi - \frac{1}{3} \cos 3\phi\right) \\ \Delta y &= \frac{3}{4} T \left(\sin \phi - \frac{1}{3} \sin 3\phi\right) \end{aligned}\right\} \tag{14}$$

$$x = \left(1 - \frac{T}{4}\right) \cos \phi + \frac{T}{4} \cos 3\phi \tag{15}$$

where the value of r has been so adjusted that the chordwise extremities of the section are at $x = \pm 1$. The thickness ratio T is defined as twice the height of the bump divided by its length 2. The bumps given by equations (14) and (15) are shown in figure 6(a) for $T = 0$, 0.1, 0.2, and 0.3. The family of symmetrical sections shown in this figure was derived by Kaplan in reference 3 by a generalization of the Joukowski transformation. The corresponding velocity distributions are shown in figure 6(b).

The velocity distribution on the wall (that is, for $|x| > 1$, $y = 0$) can be obtained from the general expression for the velocity at any point in the plane outside the section; thus, for an arbitrary airfoil situated at an angle of attack α in a free stream of unit velocity, the expression for the derivative w_z of the potential function in the airfoil z-plane is

$$w_z = \frac{w_p}{dz/dp}$$

where w_p is the derivative of the potential function in the circle p-plane. If p is written in the form

$$\left.\begin{aligned} p &= e^{\psi+i\phi} \\ R &= e^{\psi_0} \\ \Omega &= \psi - \psi_0 \end{aligned}\right\} \tag{16}$$

evaluation of w_p and dz/dp yields the following formulas for the magnitude v_z and the direction Π of the velocity vector in the airfoil plane:

$$w_z = v_z\, e^{-i\Pi}$$

$$v_z = \sqrt{\frac{\sinh^2 \Omega \cos^2 (\phi + \alpha) + \left[\cosh \Omega \sin (\phi + \alpha) + \sin (\alpha + \beta_T)\right]^2}{\left(\cosh \Omega \sin \phi - \frac{\partial \Delta x}{r \partial \phi}\right)^2 + \left(\sinh \Omega \cos \phi + \frac{\partial \Delta y}{r \partial \phi}\right)^2}} \tag{17}$$

$$\tan \Pi = \frac{\left(\sinh\Omega\cos\phi + \frac{\partial\Delta y}{r\partial\phi}\right)\left[\cosh\Omega\sin(\phi+\alpha)+\sin(\alpha+\beta_T)\right] - \sinh\Omega\cos(\phi+\alpha)\left(\cosh\Omega\sin\phi - \frac{\partial\Delta x}{r\partial\phi}\right)}{-\left\{\sinh\Omega\cos(\phi+\alpha)\left(\sinh\Omega\cos\phi + \frac{\partial\Delta y}{r\partial\phi}\right) + \left(\cosh\Omega\sin\phi - \frac{\partial\Delta x}{r\partial\phi}\right)\left[\cosh\Omega\sin(\phi+\alpha)+\sin\left(\alpha+\beta_T\right)\right]\right\}} \tag{18}$$

where β_T is the zero-lift angle.

For a symmetrical flow and section, $\alpha = \beta_T = 0$; whereas, for points on the wall, $\phi = \partial\Delta x/\partial\phi = 0$. Equation (17) thus reduces to

$$(v_z)_{wall} = \frac{\sinh \Omega}{\sinh \Omega + \left(\frac{\partial \Delta y}{r \partial \phi}\right)_{\phi=0}} \tag{19}$$

The value of $\left(\frac{\partial \Delta y}{\partial \phi}\right)_{\phi=0}$ for arbitrary $\Omega \geq 0$ is obtained by differentiating equation (12b), replacing R with e^{Ψ}, and using for a_n the values previously determined for the section.

The conformal transformation of a sinusoidal bump was next determined by the method of successive approximations outlined in the preceding section. The thickness ratio T was taken to be 0.2, so that the symmetrical section has the equation

$$y = \pm 0.1 \, (1 + \cos \pi x) \quad (-1 \leq x \leq 1) \tag{20}$$

The symmetrical section of figure 6(a) with $T = 0.2$ was chosen as the zeroth approximation. Two approximations were carried out. The maximum differences between the ordinates of the given boundary (equation (20)) and the successively derived boundaries were about 5, 1.5, and 0.25 percent for the zeroth, the first, and the second approximations, respectively. Table 2 contains the data for the second approximation and figure 7 shows the velocity distribution over bump and wall. The approximate result of Allen, obtained on the basis of thin-airfoil theory, is also shown in figure 7. The maximum difference between the two curves is about 8 percent of the maximum increment of velocity over the free-stream value. This difference, it should be remembered, is for a 20-percent thickness ratio; for the very small thickness ratios considered by Allen, thin-airfoil theory is quite adequate.

Figures 6 and 7 show that the velocity distribution in the neighborhood of the point where bump meets wall merits discussion. A symmetrical section can become tangent to the wall in any one of three ways: with infinite curvature, zero curvature, and finite nonzero curvature. The case of infinite curvature, properly called a cusp, holds for the special family of sections given by equations (14) and (15) and also for the trailing edge of a symmetrical Joukowski airfoil. The velocity curve corresponding to both bump and wall has a minimum value at the cusp; the velocity gradient at the cusp is finite on the bump side and infinite on the wall side as indicated in figure 6(b). See reference 4 for a comparison with experiment.

Zero curvature is obtained at the sharp edge of the symmetrical section if, in addition to conditions (13), the following equation holds:

$$\sum_{1}^{\infty} n^3 a_n = 0$$

The velocity curve in this case has a minimum at some point on the bump and the velocity gradient is continuous at the point where the section meets the wall.

The section obtained by reflecting the cosine bump in the wall has finite nonzero curvature at its sharp edge. The velocity is a minimum at a point on the bump, as seen in figure 7, but the continuity of the velocity gradient at the sharp edge is, from the calculations of this paper, still an open question. It is conjectured that, at a sharp edge of this type, the velocity gradient has a finite discontinuity.

EXTERIOR-INTERIOR BUMPS

The flow over a bump has been derived in the preceding section by reflection of the bump contour in the wall and analysis of the resulting symmetrical section. If an exterior-interior bump, namely, a distortion of part of a wall in both directions perpendicular to the wall, is reflected in the wall, a symmetrical figure-eight section results, as indicated in figure 8. The mapping of such a contour onto a circle can be accomplished as previously described. It appears, however, that the derivative dz/dp of the transformation will be zero at a point outside the circle corresponding to a point within the loop consisting of the interior part of the bump contour and its reflection. That such a zero must exist becomes evident upon tracing the paths around the figure-eight contour corresponding to concentric circles larger than the basic circle. As indicated schematically in figure 8, the transition contour between those of figure-eight type and those simply connected has a sharp-edged extremity at the point F inside the loop formed by the interior part of the bump contour and its reflection. At this sharp edge, $dz/dp = 0$. Although this property of a looped contour might be useful, for example, in locating the singularities of a mapping function, this method of attack does not yield the desired flow over the exterior-interior bump (the flow actually obtained is that whose zero streamline is the path ABCDEFGH in fig. 8). It may be noted that the conventional application of thin-airfoil theory also breaks down in this case.

The flow over an exterior-interior bump can be obtained by mapping the bump and the wall contours onto an infinitely long straight line. Points on the bump contour are related to points on the straight line by the CMF.

$$z - \zeta = \Delta x + i\Delta y$$

as indicated in figure 9, and points on the straight line are related to points on the unit circle by the bilinear transformation, which for the problem under consideration is taken as

$$\zeta = i\left(\frac{p - i}{p + i}\right) \tag{21}$$

Equation (21) transforms the upper half ζ-plane into the region exterior to the unit circle; corresponding points of both regions are shown in figure 9. For points on the boundaries, the inverse-power-series expression for $z - \zeta$ (equations (9) and (21)) yields

$$\left.\begin{aligned} \Delta x &= \sum_0^\infty a_n \cos n\phi + \sum_0^\infty b_n \sin n\phi \\ \Delta y &= \sum_0^\infty b_n \cos n\phi - \sum_0^\infty a_n \sin n\phi \\ x &= \xi + \Delta x = \tan\frac{90^\circ - \phi}{2} + \Delta x(\phi) \\ y &= \Delta y \end{aligned}\right\} \tag{22}$$

The velocity distribution at the surface of the bump is obtained from the complex velocity function w_z:

$$w_z = \frac{w_\zeta}{\frac{dz}{d\zeta}} = \frac{1}{\frac{dz}{d\zeta}} = \frac{1}{1 + \frac{d(z - \zeta)/dp}{d\zeta/dp}} = \frac{1}{1 - (1 + \sin\phi)\left(\frac{d\Delta x}{d\phi} + i\frac{d\Delta y}{d\phi}\right)}$$

The absolute magnitude of the velocity v is therefore given by

$$v = \frac{1}{\sqrt{\left[1 - (1 + \sin\phi)\frac{d\Delta x}{d\phi}\right]^2 + \left[(1 + \sin\phi)\frac{d\Delta y}{d\phi}\right]^2}}$$

As a simple example of an exterior-interior bump, the family represented by

$$\Delta x = b \sin \phi$$

$$\Delta y = y = b \cos \phi$$

$$x = \tan \frac{90^\circ - \phi}{2} + b \sin \phi$$

is illustrated for various values of b, together with the corresponding velocity distributions, in figures 10 and 11. By the methods previously described and also by superposition of solutions by linear combinations of CMF's, arbitrary distortions of a straight wall may be analyzed or synthesized.

CONCLUSION

The velocity distributions on corrugations and bumps as determined by conformal transformation are, in the case of 20-percent thickness ratio, appreciably different from the corresponding results by thin-airfoil theory. The maximum differences, expressed as fractions of the maximum increment of velocity over free-stream velocity produced by the disturbance, amount to approximately 16 percent for a sinusoidal corrugation of 20-percent thickness ratio and 8 percent for a sinusoidal bump of the same thickness ratio. In the limit of zero thickness ratio, the results by conformal transformation are identical with the results by thin-airfoil theory.

Aircraft Engine Research Laboratory,
National Advisory Committee for Aeronautics,
Cleveland, Ohio.

REFERENCES

1. Allen, H. Julian: Notes on the Effect of Surface Distortions on the Drag and Critical Mach Number of Airfoils. NACA ACR No. 3I29, 1943.

2. Theodorsen, Theodore: Theory of Wing Sections of Arbitrary Shape. NACA Rep. No. 411, 1931.

3. Kaplan, C.: The Flow of a Compressible Fluid Past a Curved Surface. NACA ARR No. 3K02, 1943.

4. Preston, J. H., and Sweeting, N. E.: The Experimental Determination of the Boundary Layer and Wake Characteristics of a Simple Joukowski Aerofoil, with Particular Reference to the Trailing Edge Region. F. M. 570, S. & C. 1499, Ae. 2168, (British), March 1943.

TABLE 1. - CMF AND VELOCITY DISTRIBUTION FOR COSINE CORRUGATION

ϕ (radians)	ψ	ϵ	θ	$\frac{d\psi}{d\phi}$	$\frac{d\epsilon}{d\phi}$	v	v (thin-airfoil theory, reference 1)
0	-0.3142	0	0	0	-0.4412	0.6939	0.6858
$\pi/12$	-.2925	-.1118	.3736	.1607	-.3996	.7098	.7075
$\pi/6$	-.2343	-.2038	.7274	.2729	-.2971	.7544	.7654
$\pi/4$	-.1551	-.2659	1.0513	.3228	-.1776	.8191	.8440
$\pi/3$	-.0693	-.2981	1.3453	.3272	-.0718	.8924	.9298
$5\pi/12$	.0141	-.3054	1.6144	.3068	.0128	.9673	1.0137
$\pi/2$	.0904	-.2930	1.8638	.2747	.0789	1.0404	1.0907
$7\pi/12$	.1573	-.2652	2.0978	.2354	.1315	1.1113	1.1580
$2\pi/3$	.2133	-.2253	2.3197	.1916	.1716	1.1760	1.2139
$3\pi/4$	.2573	-.1762	2.5324	.1447	.2013	1.2320	1.2576
$5\pi/6$	.2889	-.1208	2.7387	.0966	.2207	1.2736	1.2890
$11\pi/12$	.3079	-.0613	2.9411	.0482	.2320	1.2996	1.3079
π	.3142	0	3.1416	0	.2353	1.3077	1.3142

National Advisory Committee
for Aeronautics

TABLE 2. - CMF AND VELOCITY DISTRIBUTION FOR COSINE BUMP

ϕ (radians)	Ω	Δx	Δy	x	$\frac{\partial \Delta x}{\partial \phi}$	$\frac{\partial \Delta y}{\partial \phi}$	v
$\pi/2$	0	0	0.2000	0.	0.3064	0	1.3901
$4\ \pi/9$	0	-.0523	.1910	.1373	.2866	.1021	1.3522
$7\ \pi/18$	0	-.0978	.1651	.2756	.2282	.1907	1.2509
$\pi/3$	0	-.1299	.1262	.4159	.1347	.2486	1.1149
$5\ \pi/18$	0	-.1436	.0814	.5581	.0217	.2538	.9801
$2\ \pi/9$	0	-.1386	.0413	.6977	-.0718	.1963	.8793
$\pi/6$	0	-.1033	.0149	.8422	-.1054	.1063	.8272
$\pi/9$	0	-.1053	.0031	.9207	-.0815	.0350	.8183
$\pi/18$	0	-.0949	.0002	.9803	-.0373	.0044	.8354
$\pi/36$	0	-.0925	.0000	.9951	-.0173	.0006	.8461
0	.05	-.0915	0	1.0016	0	.0093	.8547
0	.10	-.0908	0	1.0064	0	.0178	.8598
0	.20	-.0883	0	1.0253	0	.0318	.8735
0	.30	-.0846	0	1.0566	0	.0416	.8889
0	.40	-.0801	0	1.1001	0	.0476	.9040
0	.50	-.0752	0	1.1559	0	.0508	.9180
0	.60	-.0700	0	1.2242	0	.0518	.9306
0	.70	-.0649	0	1.3055	0	.0513	.9417
0	.80	-.0598	0	1.4003	0	.0497	.9512
0	.90	-.0550	0	1.5096	0	.0474	.9594
0	1.00	-.0503	0	1.6343	0	.0448	.9663

National Advisory Committee
for Aeronautics

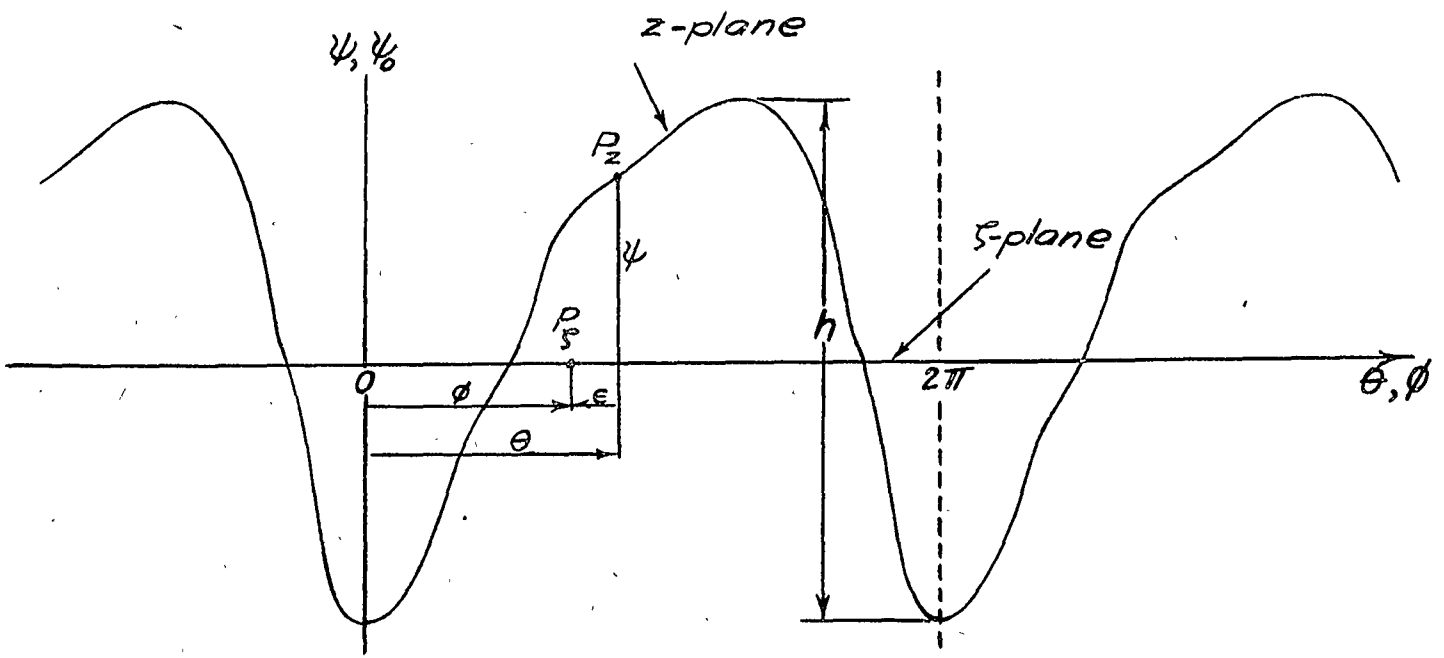

NATIONAL ADVISORY
COMMITTEE FOR AERONAUTICS

Figure 1. - Conformal transformation of a corrugated surface.

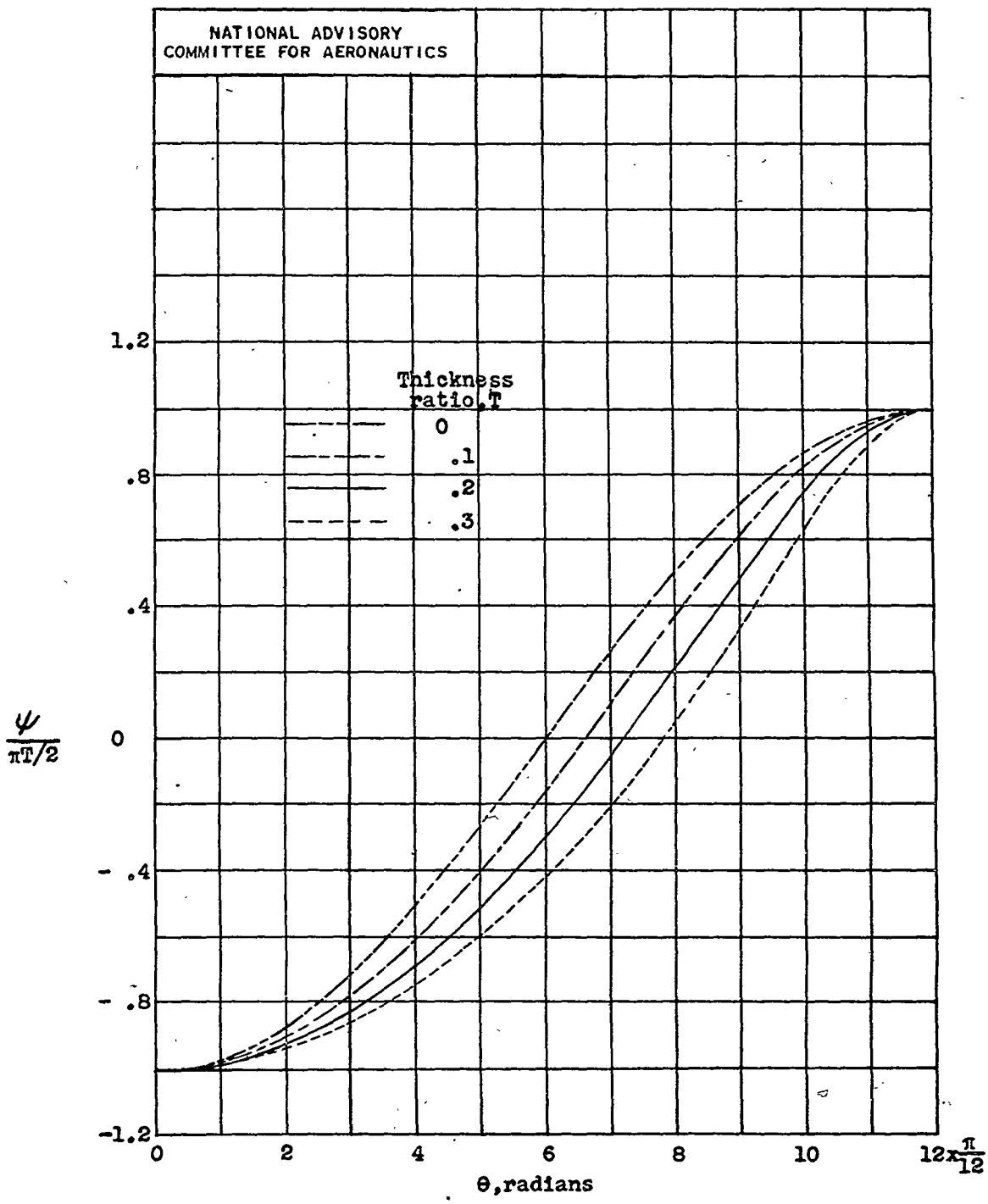

Figure 2.- Special family of corrugations.

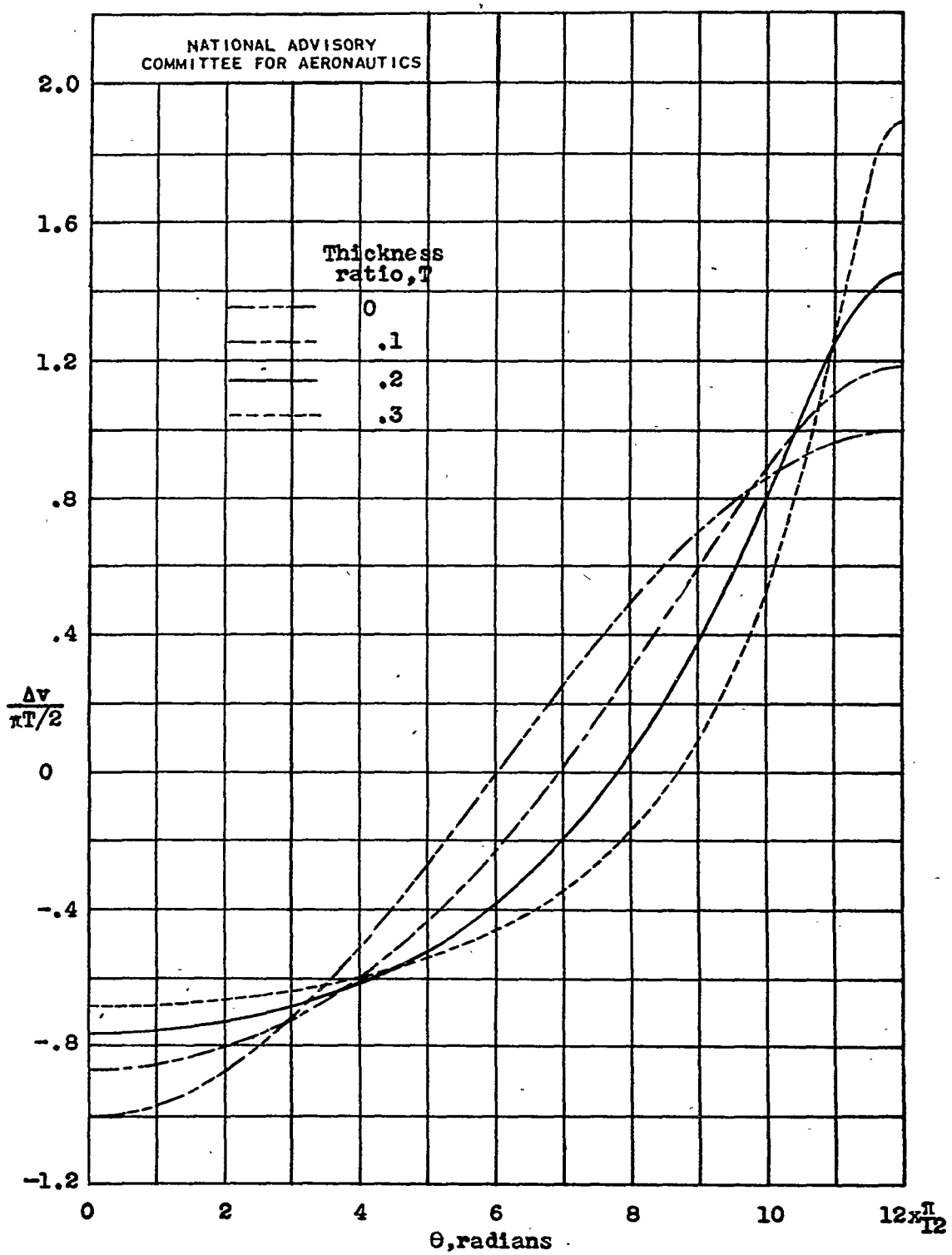

Figure 3.- Velocity distributions of special family of corrugations.

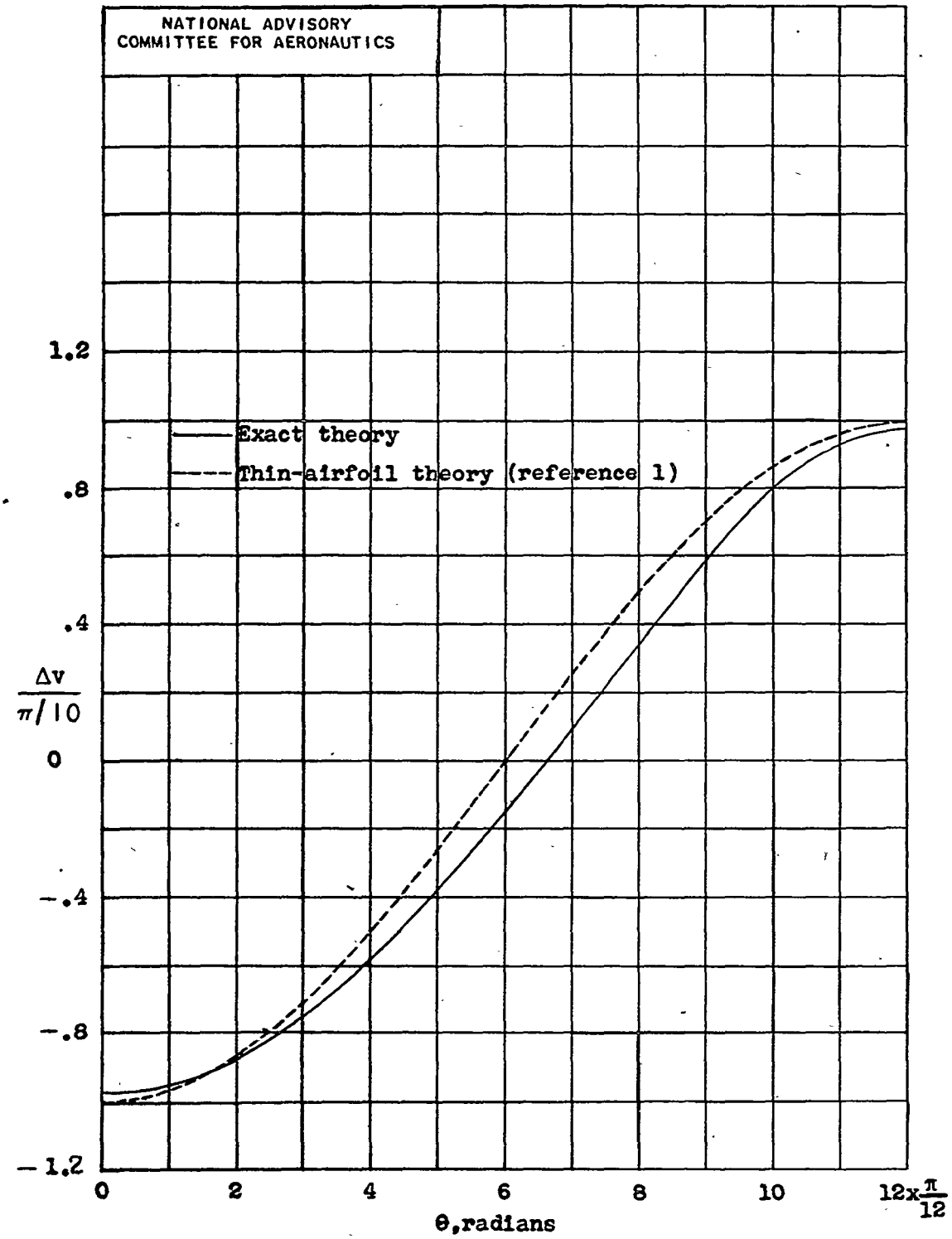

Figure 4.- Comparison of velocity distributions for cosine corrugations.

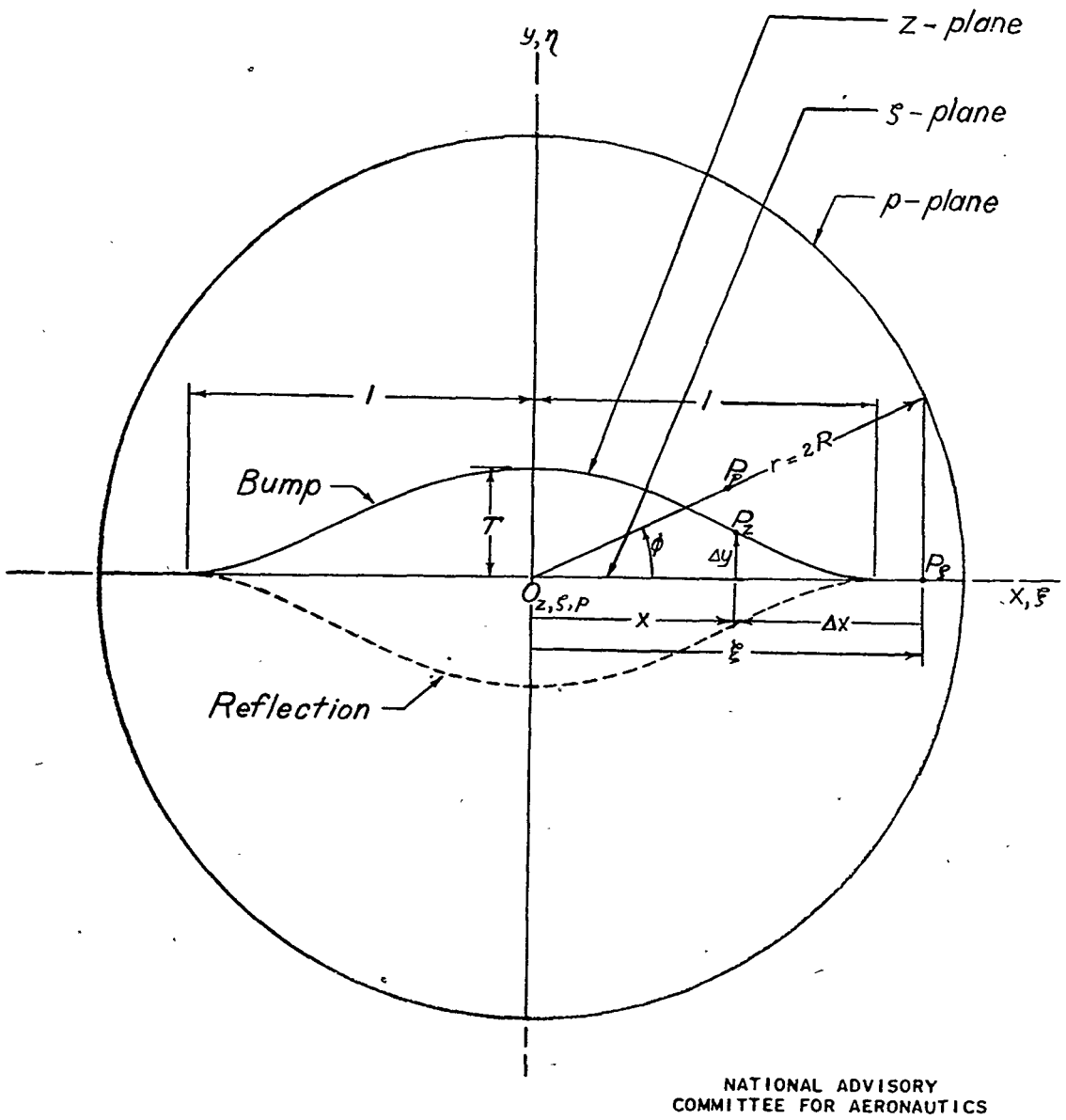

Figure 5. – Conformal transformation of a symmetrical section.

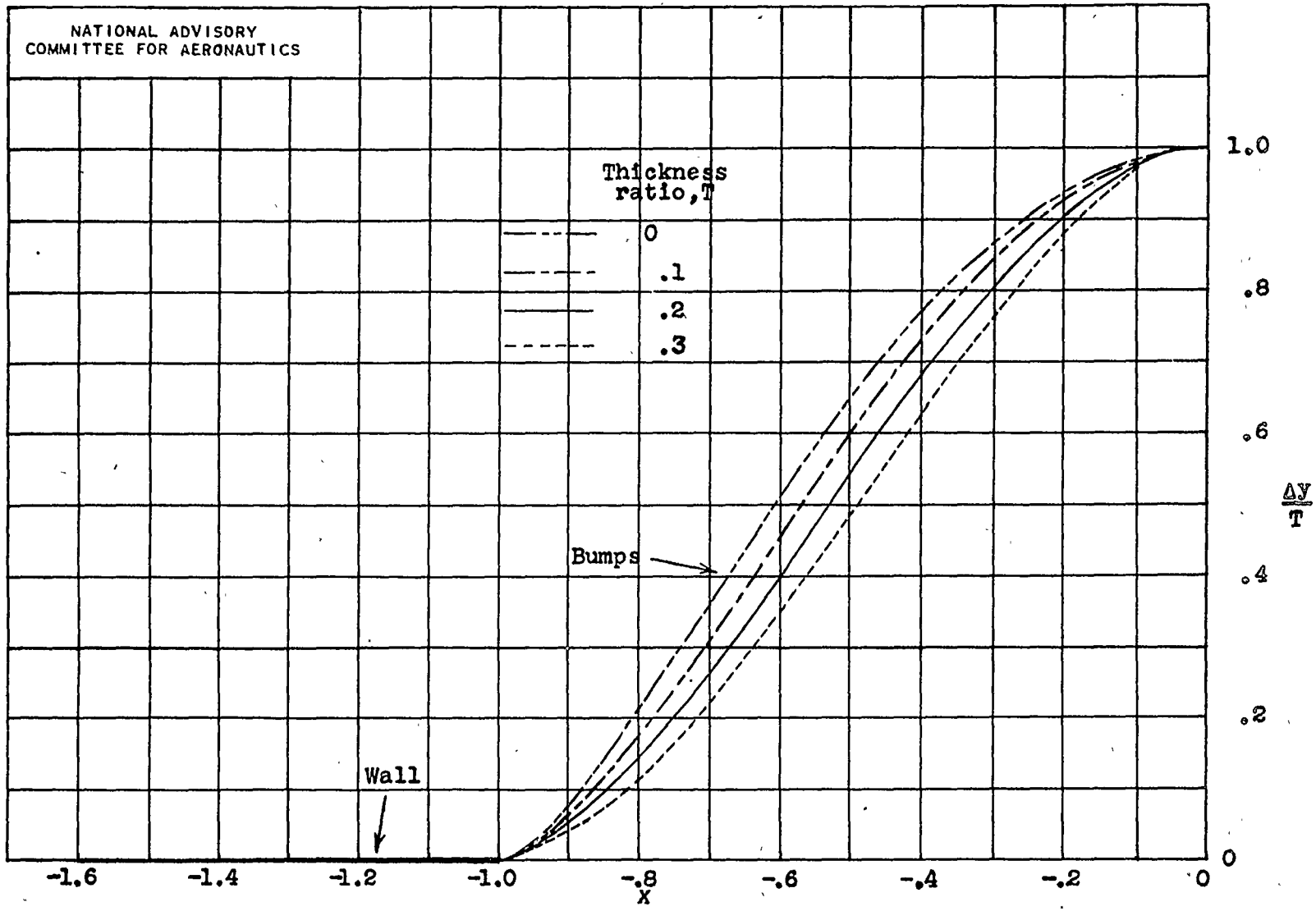

(a) Profiles.

Figure 6.- Special family of bumps.

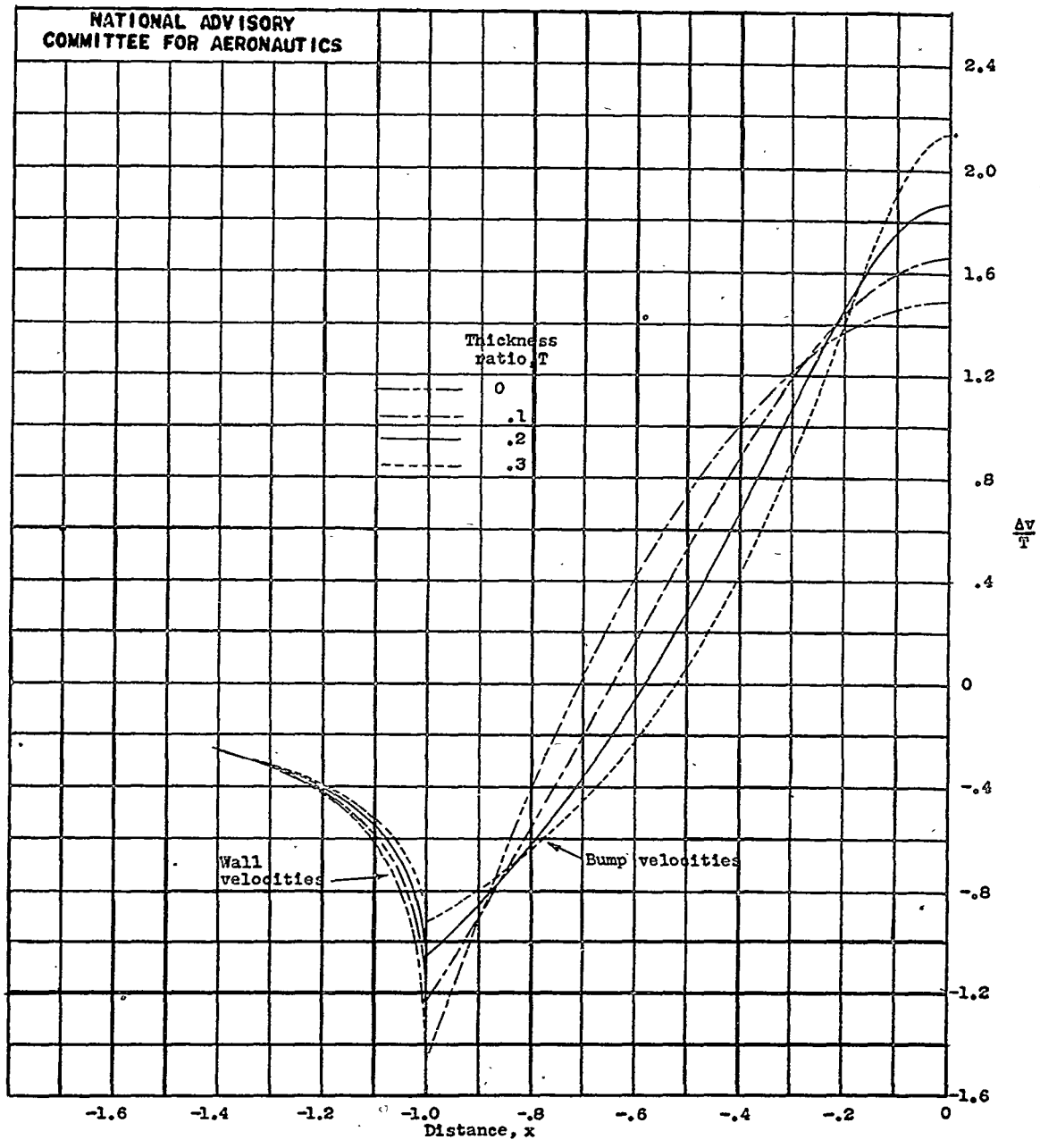

(b) Velocity distributions.
Figure 6.- Concluded.

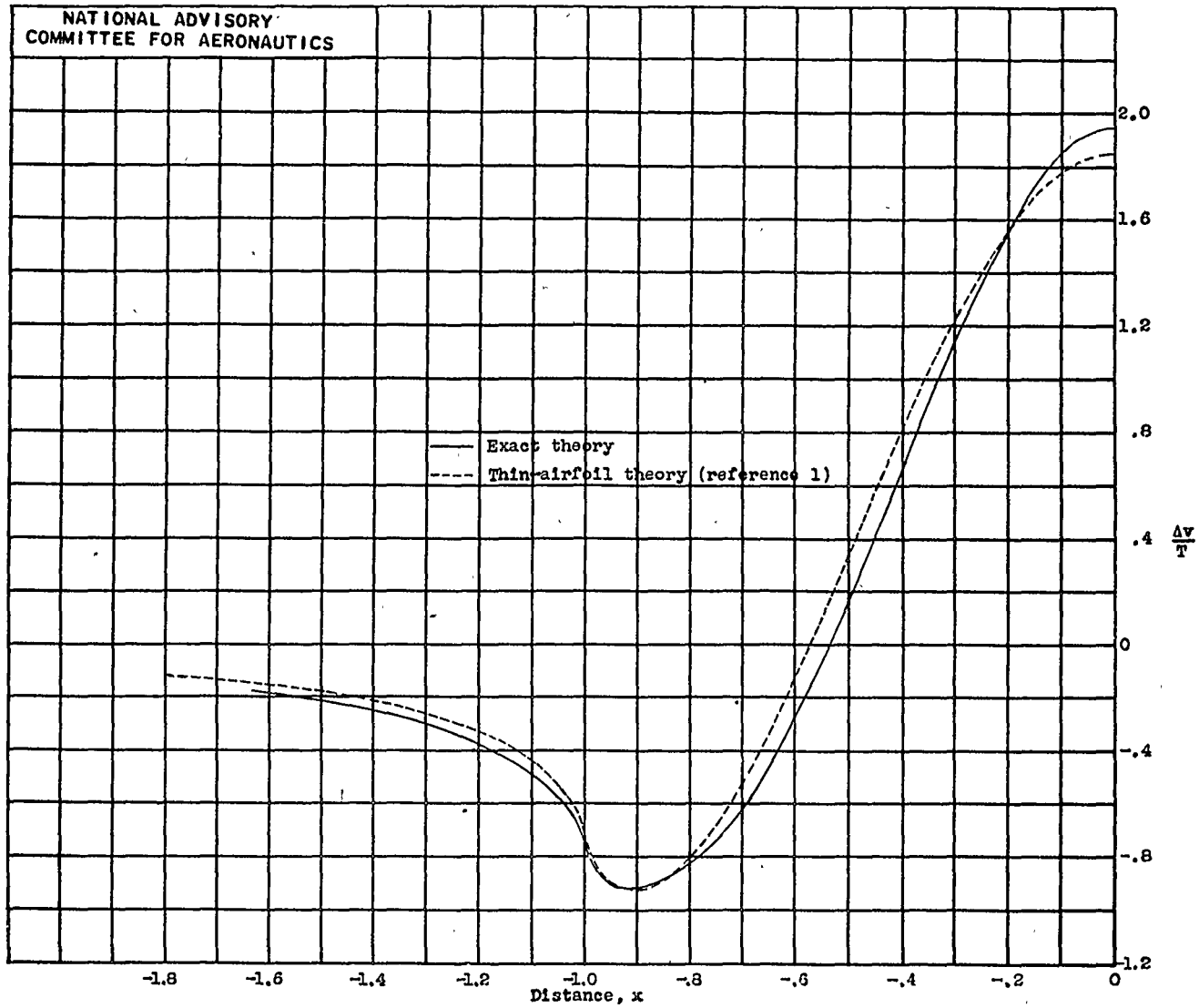

Figure 7. - Comparison of velocity distributions for cosine bumps.

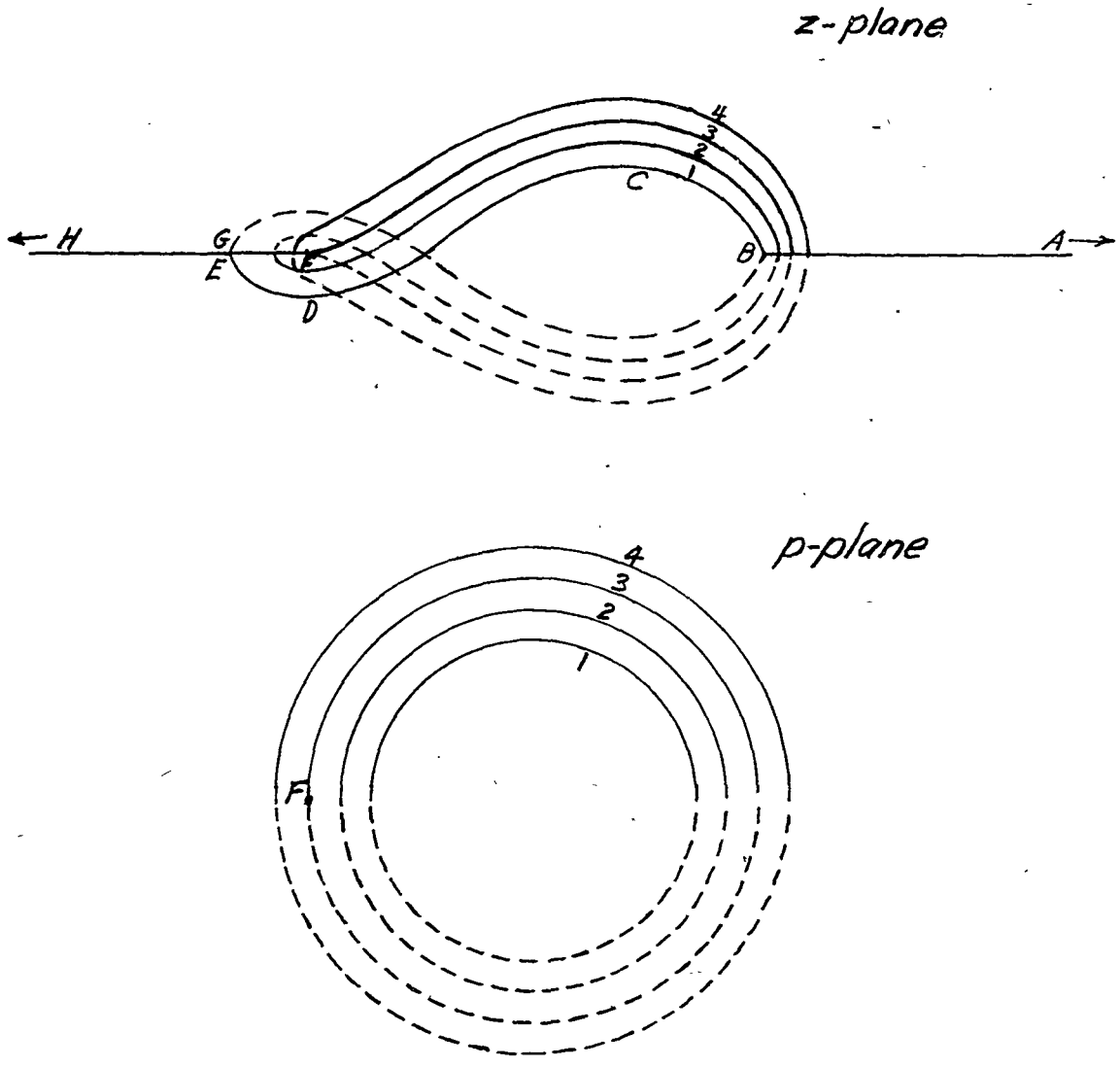

NATIONAL ADVISORY
COMMITTEE FOR AERONAUTICS

Figure 8.—Mapping of figure-eight contour.

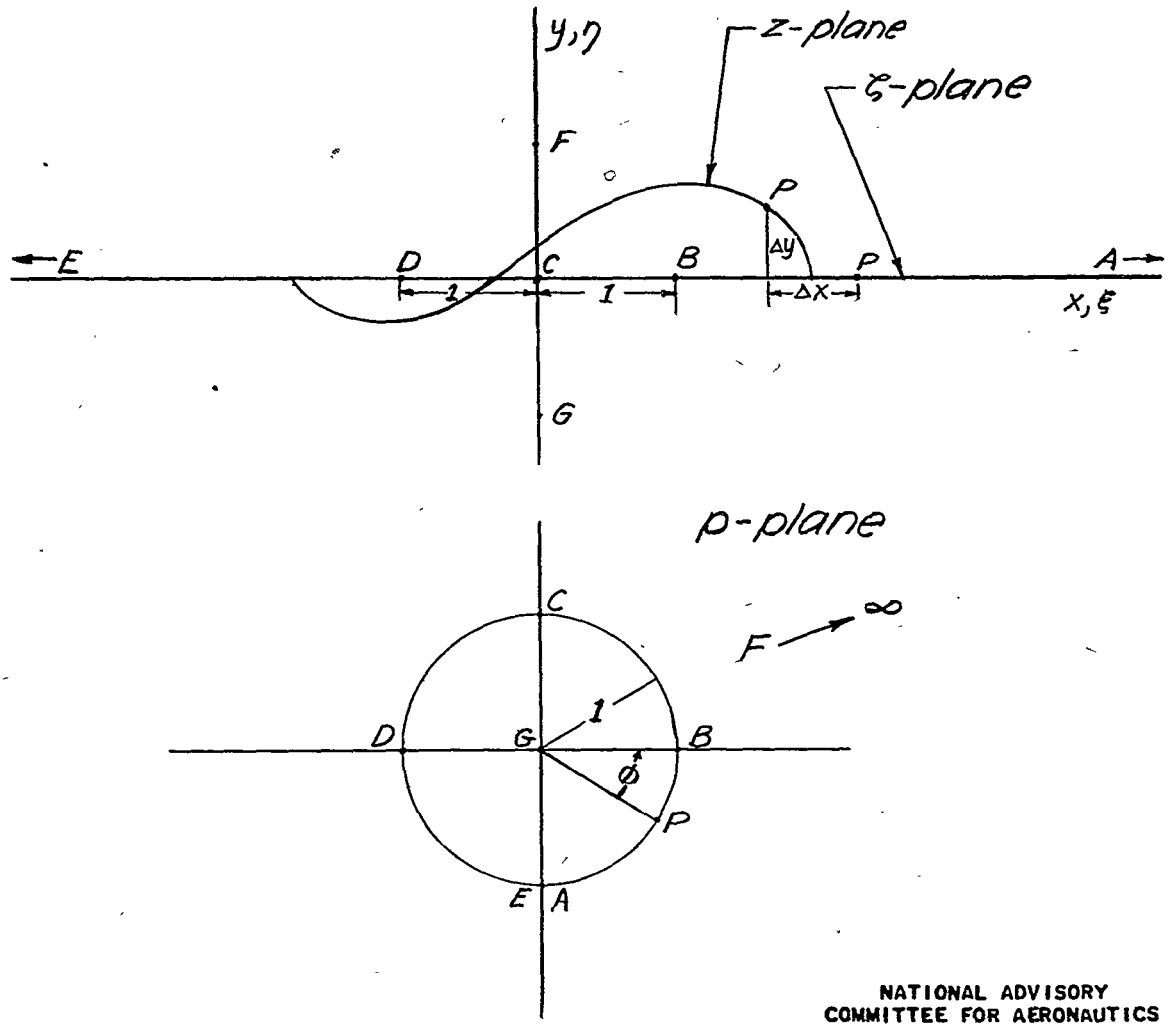

Figure 9.—Mapping of bump using bilinear transformation.

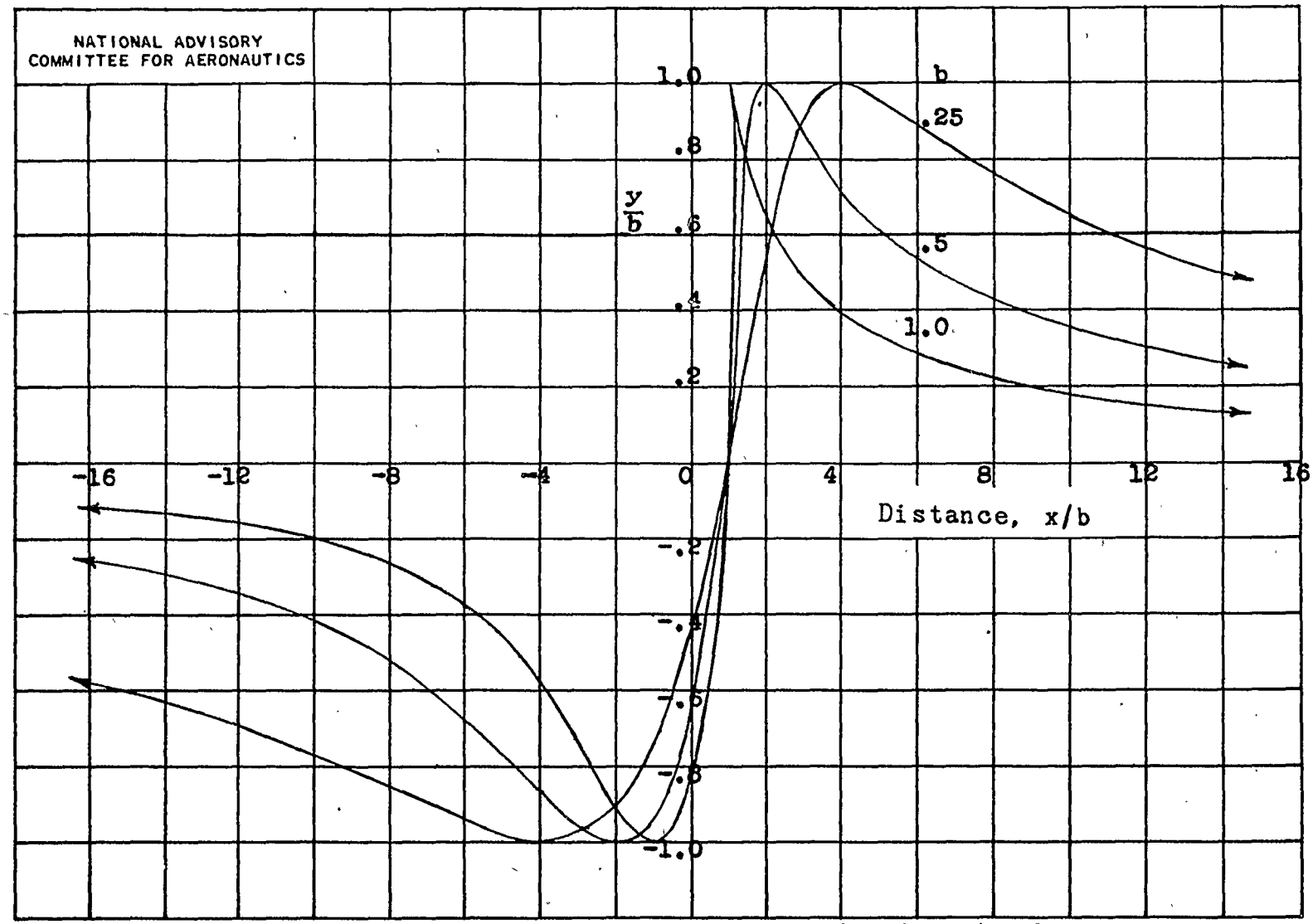

Figure 10.- Special family of infinitely extended exterior-interior bumps.

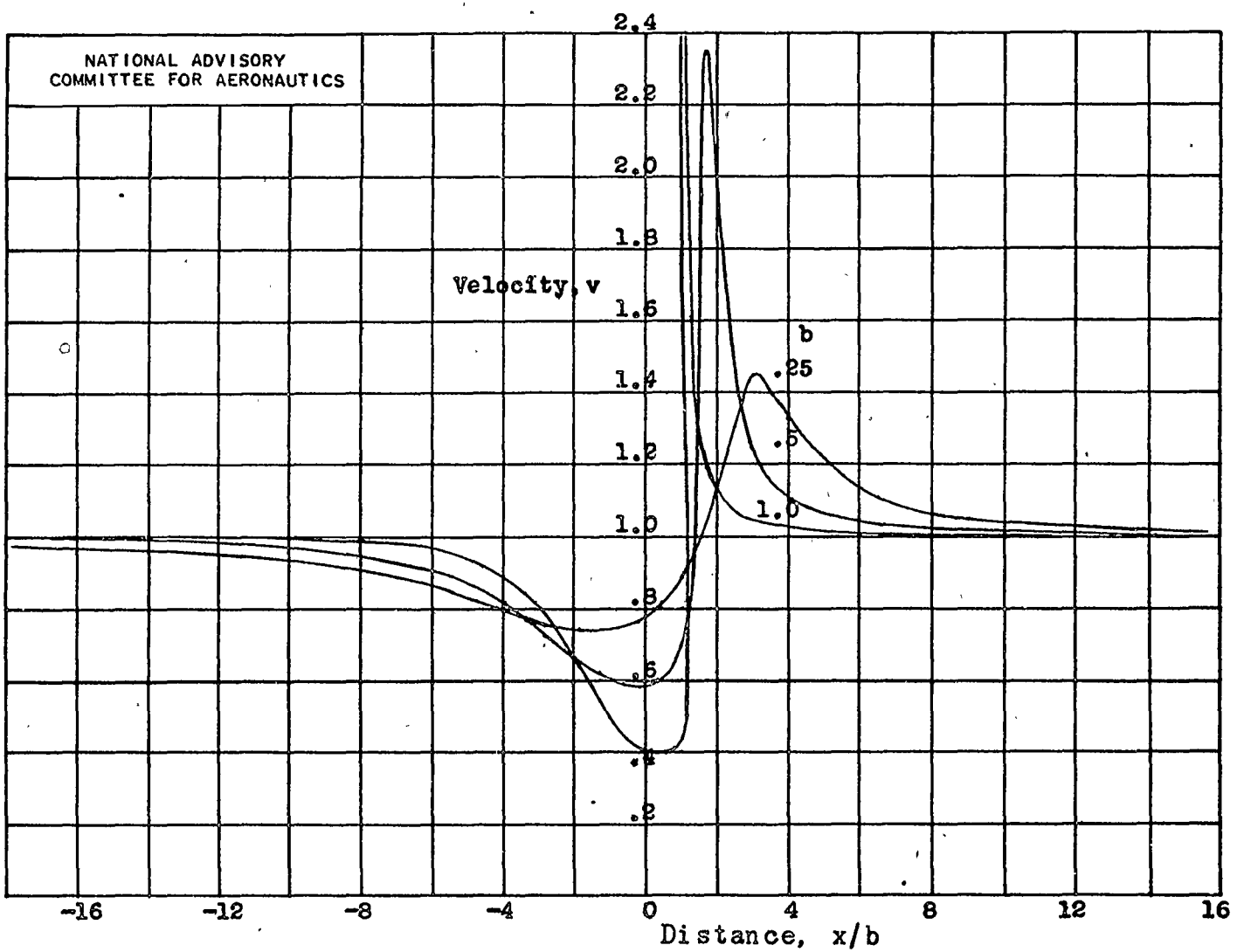

Figure 11.- Velocity distributions of special family of infinitely extended exterior-interior bumps.